ARMA 13-241

# Effect of confining pressure on permeability during deformation and failure of several rocks under compression

Alam A.K.M. B., Niioka M., Fujii Y.

*Rock Mechanics Laboratory, Faculty of Engineering, Hokkaido University, Japan*



This paper was prepared for presentation at the 47th US Rock Mechanics / Geomechanics Symposium held in San Francisco, CA, USA, 23-26 June 2013.



**ABSTRACT:** Triaxial test was carried out under confining pressure of 1-15 MPa at 22°C by using an ultra compact triaxial cell on Shikotsu welded tuff, Kimachi sandstone and Inada granite. The permeability was measured by using constant flow or transient pulse method. In case of tuff with increasing stress, permeability decreased to residual strength state. In case of sandstone permeability began to decrease, reached minima before peak stress, began to increase again and reached almost stable value under residual strength state; The permeability from consolidation to residual strength state increased under 1 MPa, was almost the same values under 5-10 MPa with some exceptions, it decreased under 11-15 MPa. For granite, the permeability and stress relationship was the same as sandstone; The permeability ratio of consolidation to residual strength decreased with increasing confining pressure up to 9 MPa, afterward the permeability began to increase under 11-15 MPa. From the experimental results, sealability can be improved in EdZ for all the rocks. For tuff improvement of sealability can also be expected in EDZ; for sandstone it is achievable if enough support pressure is applied but for granite it cannot be expected.

## 1. INTRODUCTION

Around underground excavations, there occur the Excavation disturbed Zone (EdZ) and Excavation Damaged Zone (EDZ) due to excavation activities [1]. The porosity and permeability may increase or decrease i.e., sealabiliy may deteriorate or improve in these zones [1, 2]. Rock, before or around peak stress under triaxial compression can be recognized as EdZ or EDZ as shown in Fig. 1. The objective of this study is to clarify the confining pressure effect on permeability behavior considering a wide range of rocks i.e., Shikotsu welded tuff, Kimachi sandstone, and Inada granite as HM processes under compression.

## 2. EXPERIMENT

### *2.1 Specimen and Sample Preparation*

Three types of rock block were considered and the properties are in Table 1. Firstly, the P-wave velocity of the rock blocks was measured with 140 kHz sensors to know the anisotropy, and core boring was carried out in the direction of the slowest P-wave velocity. Finally, the core specimens having the diameter of 30 mm and 60 mm in length with parallelism of 2/100 were prepared from these rock blocks.

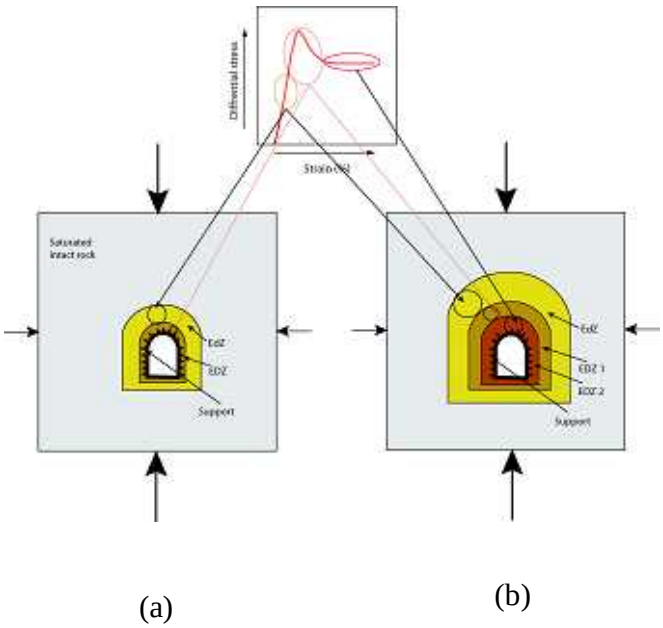


Fig. 1. EdZ and EDZ around an excavation. (a) Initial state (b) Final (residual strength) state.

Table 1. Rock blocks and properties are shown as "value (number of specimen) ± standard deviation"

| Name of rock | Effective porosity (%) | UCS (saturated) (MPa) |
|---|---|---|
| Shikotsu welded tuff | 35.6 (2) ± 1.65 | 13.53 (2) ± 2.74 |
| Kimachi sandstone | 18.35 (2) ± 1.98 | 20.53 (2) ± 2.35 |
| Inada granite | 0.63 (2) ± 0.05 | 180.85 (2) ± 16.93 |

Afterward, the specimens were made fully pure water saturated. Two stainless steel end-pieces, having a central hole to allow the flow of water through the specimen were attached with each saturated specimen by vinyl tape, and two cross type strain gauges were glued to the center of the opposite sides of the specimen to have strain measurements. Silicone sealant was coated on the specimen and the end-pieces attached specimen was jacketed with heat shrinkable tube. Then the sample was kept in water for 24 hours.

### *2.2 Experimental Setup*

For the triaxial experiment, an ultra compact triaxial cell and two stainless steel attachments (upper and lower) having the facilities of water flow as well as pore pressure measurements were used for the experiment (Fig. 2 (a)). The constant flow of water and pore pressure measurement within the end-pieces attached sample were maintained by using a syringe pump which was connected to the lower attachment. In constant flow method, the upper attachment was open to the atmosphere for drainage of water (Fig. 2 (a)). For transient pulse method, the upper attachment was connected to an accumulator (Fig. 2 (c)) and the syringe pump acted as another accumulator for downstream. Axial stress was applied by a loading frame whereas the confining pressure was maintained by a double ball plunger pump with a relief valve.

### *2.3 Experimental Procedure*

The saturated sample was inserted into the triaxial cell. Then the upper and lower attachments were attached with it. Afterward the axial stress and confining pressure were introduced.

In the triaxial test, confining pressure ($P_c$) was used to make $\sigma_2 = \sigma_3$ and the axial stress ($\sigma_A$) acted as $\sigma_1$ (Figure 3(a)). In consolidation state, the axial stress was equal to the confining pressure, by making the stress situation as $\sigma_1 = \sigma_2 = \sigma_3$. To reach the desired consolidation pressure the axial stress was increased first, then the confining pressure was applied, up to the target consolidation pressure (Figure 3(b)).

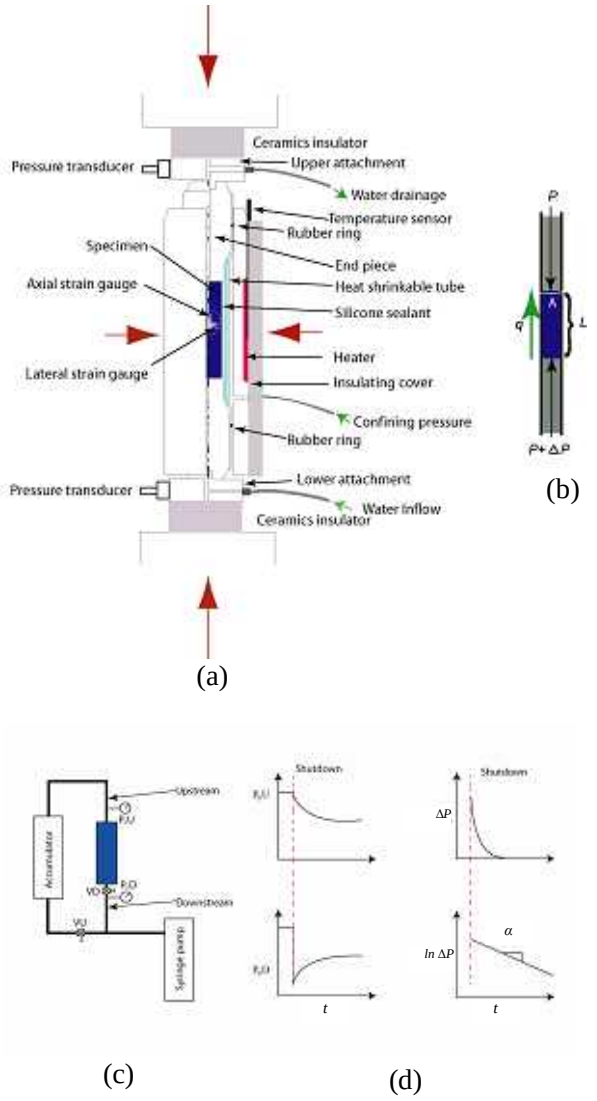


Fig. 2. Experimental setup. (a) Ultra compact triaxial cell and accessories for constant flow method (b) Basis for permeability measurement in constant flow method. (c) Schematic diagram for transient pulse method (d) $\alpha$- gradient of time-ln $\Delta P$ in transient pulse method.

After reaching the target consolidation pressure, it was kept in this condition for 24 hours at 22°C temperature by using air conditioner. On the consolidated samples, constant strain rate controlled compression was introduced at a rate of $10^{-5}$ $s^{-1}$ (0.036 mm/min) until the axial strain reached to 10% for tuff and 7% for sandstone and granite.

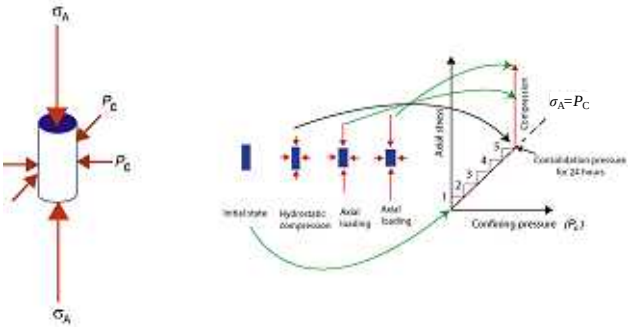


(a) (b)

Fig. 3. The triaxial test and the experimental procedure. (a)The triaxial text (b) Procedure to reach the target consolidation pressure and compression.

### *2.4 Permeability Measurement*

Constant flow of pure water at a rate of 0.3 ml/min was maintained in the axial direction by using the syringe pump during the period of the consolidation and compression in constant flow method for Shikotsu welded tuff. The permeability $K$ ($m^2$) was calculated by the following equation.

$$K = \frac{q \cdot \mu}{A} \cdot \left( \frac{dP}{dL} \right)^{-1}$$

where $q$: flow rate ($m^3$/s), $\mu$: fluid viscosity (pa·s), $A$: cross sectional area ($m^2$) and d$P$/d$L$: pressure gradient (Pa/m).

The permeability of Kimachi sandstone and Inada granite was measured by the transient pulse method. The measurement was conducted at a stroke interval of 0.2 mm up to the peak load and 0.6 mm after peak load. In this case, pore pressure of 1 MPa was maintained in the whole system during consolidation and compression. At the point of permeability measurements, the valve which was connected to the accumulator was closed (Fig. (c)) and 0.5MPa pore pressure was applied in the downstream and waited for 30 min. From the gradient of time-ln ΔP (Fig. 2(d), permeability was calculated by using the following equation considering the approximate solution of Brace [3].

$$K = \frac{\mu L \alpha}{(G_1 + G_2)A}$$

Where $K$: permeability ($m^2$), $\mu$: viscosity (pa·s), $L$: length of the specimen (0.06 m), $\alpha$: gradient of the time-ln $\Delta P$ curve ($s^{-1}$), $G_1$ and $G_2$: stiffness of the hydraulic system of upstream and downstream (pa/$m^3$), $A$: cross-sectional area ($m^2$).

## 3. RESULTS

### *3.1 Shikotsu welded tuff*

In case of tuff, with increasing stress permeability decreased having slight disturbance around the peak load due to rapid volumetric change (Fig. 4).

Before compression (at the end of 24 hrs. consolidation), permeability under 15 MPa was the lowest (Fig. 5(a)). In residual strength state, permeability under 1 MPa was

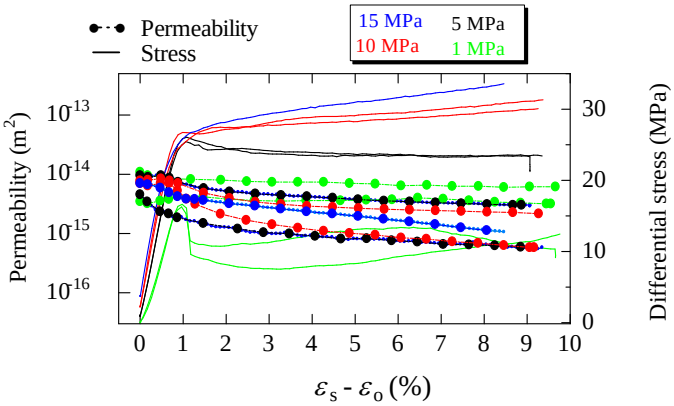


Fig. 4. Stress and permeability relation of Shikotsu welded tuff.

larger. No apparent confining pressure dependency was observed for other conditions (Fig. 5(b)). The permeability ratio of consolidation to residual strength state, showed a smaller decrease for 1 MPa and for other confining pressures the decrease magnitude was almost same (Fig. 5(c)).

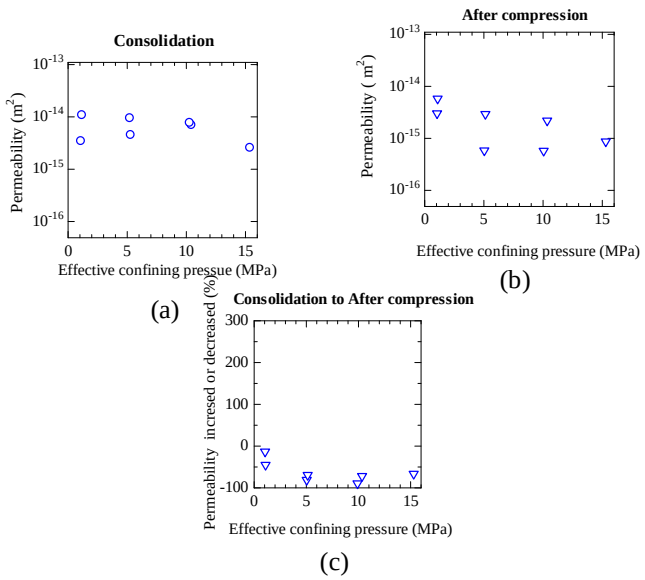


Fig. 5. Permeability after consolidation (a), after compression (b) and it's changes (c) of Shikotsu welded tuff.

### *3.2 Kimachi Sandstone*

In case of sandstone, with increasing stress, permeability began to decrease and reached to minima before peak stress. Afterward it began to increase. Under residual strength state, the permeability reached almost at a stable value (Fig. 6).

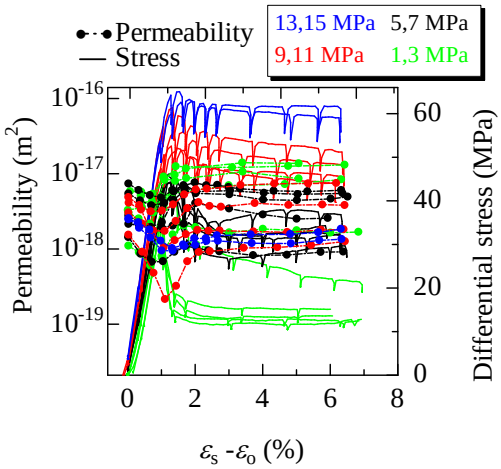


Fig. 6. Stress and permeability relation of Kimachi sandstone.

Before compression (at the end of 24 hrs. consolidation), the permeability under confining pressure of ≥ 7 MPa was slightly smaller than under confining pressure of ≤ 5 MPa (Fig. 7(a)). After 7 MPa the minima was smaller than under confining pressure of ≤ 5 MPa (Fig. 7(b)). In residual strength state, with increasing confining pressure permeability decreased (Fig. 7(c)).

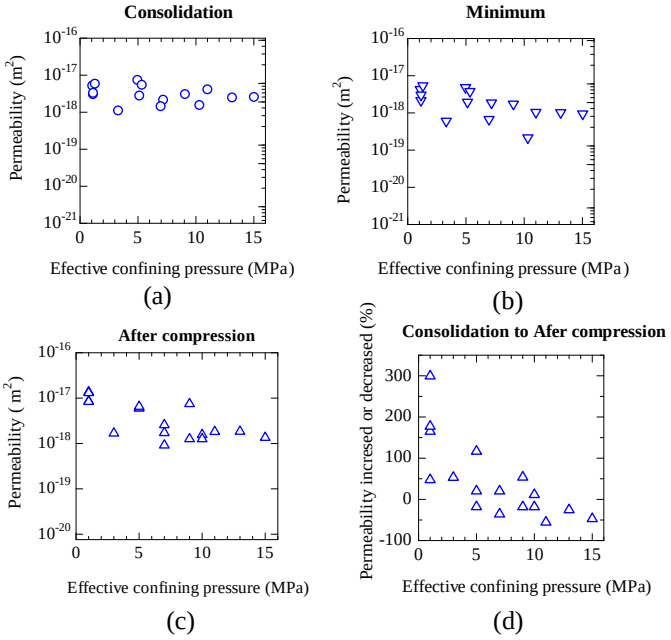


Fig. 7. Permeability after consolidation (a), at minimum (b), after compression (c) and it's changes (d) of Kimachi sandstone.

The permeability ratio of consolidation to residual strength state suggests that permeability increased under 1 MPa, showed almost the same value under 5-10 MPa with some exceptions, under 11-15 MPa it decreased (Fig. 7(d)).

### *3.3 Inada Granite*

In case of granite, with increasing stress, permeability began to decrease and reached to minima before peak stress, afterward it began to increase as sandstone. Under residual strength state, it was almost at a stable value (Fig. 8).

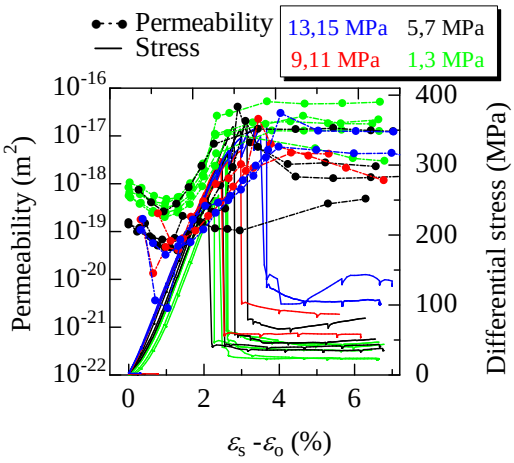


Fig. 8. Stress and permeability relation of Inada granite

Before compression, the permeability decreased with increasing confining pressure (Fig. 9(a)). The minima value of permeability decreased with increasing confining pressure (Fig. 9(b)). In residual

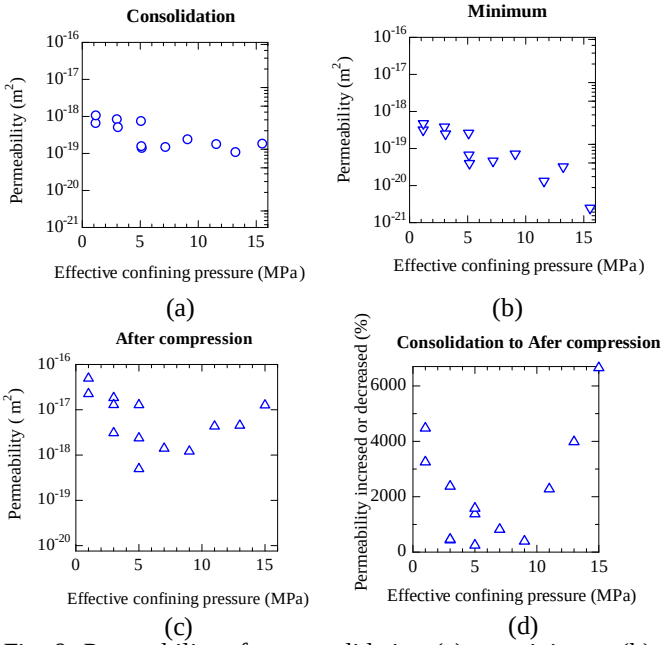


Fig. 9. Permeability after consolidation (a), at minimum (b), after compression (c) and it's changes (d) of Inada granite.

strength state, permeability decreased till confining pressure of ≥ 9 MPa, and afterward it increased again (Fig. 9(c)).

The permeability of consolidation to residual strength state decreased with increasing confining pressure up to 9 MPa. Afterward it began to increase under confining pressure of 11-15 MPa (Fig. 9(d)).

## 4. DISCUSSION

In case of of Shikotsu welded tuff, continuous decrease of permeability was observed with increasing stress. The reasons behind it would be the pore collapse and crushing of grains by compression as the rock is very porous and weak.

The decrease of permeability before peak stress was observed for Kimachi sandstone and Inada granite might be because of microcrack closure, those were not parallel to the loading axis (Fig. 10). The increase of permeability after the minima was obviously due to initiation and growth of microcracks in the loading (water flow) direction.

Plastic deformation of clay mineral could be one of the mechanisms of the confining pressure dependant permeability for Kimachi sandstone. On the other hand, elastic deformation would be one of the mechanisms for Inada granite. Sub rupture planes which might appear due to the rough and hard main rupture plane would be the reason of increased permeability in high confining pressures for Inada granite.

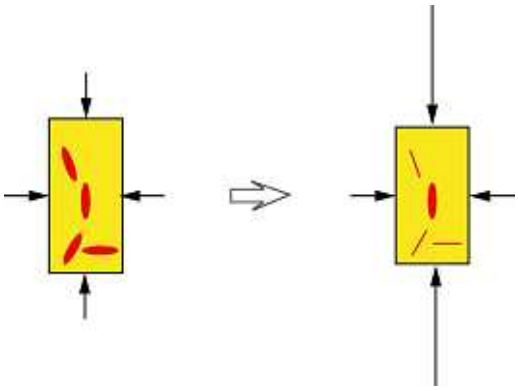

Fig. 10. Permeability decreased before peak stress due to closure of microcracks which are not parallel to the loading axis.

## 5. CONCLUSION

The experimental results under 22°C can be summarized as follows.

In the case of tuff, with increasing stress, permeability decreased with slight disturbance around the peak load; in the residual strength state, permeability under confining pressure of 1 MPa was larger and no apparent confining pressure dependency was observed for other conditions but decreased for all cases.

In the case of sandstone, with increasing stress, permeability began to decrease and reached to minima before peak stress, afterward permeability began to increase and under residual strength state, permeability reached almost stable value; in residual strength state, permeability decreased with increasing confining pressure. The permeability from consolidation to residual strength state increased, under confining pressure of 1 MPa, showed almost the same under 5-10 MPa with some exceptions, and it decreased under 11-15 MPa.

For granite, the permeability and stress relationship was the same as sandstone but in residual strength state, permeability decreased till confining pressure of ≥ 9 MPa, afterward it increased. The permeability ratio of consolidation to residual strength decreased with increasing confining pressure up to 9 MPa, afterward it began to increase under confining pressure of 11-15 MPa.

From the experimental results, considering stress redistribution, it can be stated that sealability can be improved in EdZ for all the rocks. For tuff, improvement of the sealability can be expected in EDZ; for sandstone, sealability improvement is also expected in EDZ if enough support pressure is applied, but for granite, sealability improvement in EDZ cannot be expected. These findings could contribute in rational design for construction and maintenance of tunnels and waste disposal repositories, although the authors recognize that rupture planes of a rock specimen are different from natural fractures and/or joints in rock mass and further considerations are required.

The CT imaging and microstructural analysis of the specimens after axial compression, already have been carried out. The results of the analyses as well as those of experiments under 80°C will be published in near future.

## ACKNOWLEDGEMENT

A part of this work was supported by KAKENHI (22560804).

## REFERENCES

1. Tsang, C.-F., F. Bernier, C. Davies. 2005. Geohydromechanical processes in the excavation damaged zone in crystalline rock, rock salt, and

indurated and plastic clays-in the context of radioactive waste disposal. *International Journal of Rock Mechanics & Mining Sciences* 42, 109-125.

2. Fujii Y., Y. Ishijima, Y. Ichihara, T. Kiyama. S. Kumakura, M. Takada, T. Sugawara, T. Narita, J. Kodama, M. Sawada, E. Nakata. 2011. Mechanical properties of abandoned and closed roadways in the Kushiro Coal Mine, Japan. *International Journal of Rock Mechanics & Mining Sciences* 48, 585-596.

3. Brace W. F., J. B. Walsh, W. T. Frangos. 1968. Permeability of granite under high pressure. *Journal of Geophysical Research* 73, 2225- 2236.